Japanese Journal of Applied Physics
Vol. 44, No. 8, 2005, pp. 6204–6207

Temperature-Dependent Photoluminescence of Highly Strained InGaAsN/GaAs Quantum Wells ($\lambda = 1.28$–$1.45\,\mu$m) with GaAsP Strain-Compensated Layers

Fang-I LAI, Hao-Chung KUO*, Ya-Hsien CHANG, Min-Ying TSAI, Chia-Pu CHU, Shou-Yi KUO, Shing-Chung WANG, Nelson TANSU[1], Jeng-Ya YEH[2] and Luke J. MAWST[2]

Department of Photonics and Institute of Electro-Optical Engineering, National Chiao Tung University, 1001, Ta-Hsueh Road, Hsinchu, Taiwan 30050, R.O.C.
[1]*Center for Optical Technologies, Department of Electrical and Computer Engineering, Lehigh University, 27 Memorial Drive West, Bethlehem, PA 18015, U.S.A.*
[2]*Reed Center for Photonics, Department of Electrical Computer Engineering, University of Wisconsin-Madison, 2414 Engineering Hall, 1415 Engineering Drive, Madison, WI 35706-1691, U.S.A.*

(Received September 17, 2004; accepted May 10, 2005; published August 5, 2005)

The effects of nitrogen incorporation into the $In_{0.4}Ga_{0.6}As_{1-x}N_x$/GaAs single quantum wells (SQWs), where $x = 0.5$ and 2%, grown on GaAs substrates by metalorganic chemical vapor deposition (MOCVD) were investigated using photoluminescence (PL) and high-resolution transmission electron microscopy (HRTEM). The evolution of the excitation-dependent PL and PL-peak position with temperature between 10 and 300 K shows that quantum-dot-like states occurred at that high nitrogen incorporation ($x = 2\%$) and were confirmed by an HRTEM image which showed small dark regions about 2–3 nm in size was found in the interface of $In_{0.4}Ga_{0.6}As_{0.98}N_{0.02}$ and GaAs. Our investigations indicate that high nitrogen incorporation into the $In_{0.4}Ga_{0.6}As_{1-x}N_x$/GaAs system influenced carrier localization and might cause the formation of the dot-like states.
[DOI: 10.1143/JJAP.44.6204]

KEYWORDS: InGaAsN, 1.3 μm, VCSEL, quantum-dot-like state, strain compensation

1. Introduction

Long-wavelength vertical cavity surface-emitting lasers (VCSELs) are essential devices in optical fiber metropolitan-area networks (MAN).[1)] The InGaAsN quaternary alloy system has attracted considerable interest in recent years due to its ability to grow on GaAs substrates and because of its emission in the 1.3–1.55 μm wavelength range.[2,3)] The large conduction band offset leads to an improvement in temperature performance greater than that of conventional InP-based materials.[4,5)] The GaAs system can be used in high-performance AlGaAs/GaAs distributed Bragg reflector (DBR) mirrors and enables the use of the well-established oxide-confined GaAs-based VCSEL manufacturing infrastructure.[6,7)] However, the lasing wavelength of most InGaAsN-based lasers is limited to approximately 1.3 μm, because of difficulties in growing high-quality InGaAsN/GaAs quantum-well (QW) structures with high content of In or N. First, for difficulty in growing high content of In, a higher In composition increases the compressive strain to a critical point at which the structural quality of the layer undulation of the interfaces begins to show plastic relaxation;[8)] Second, for difficulties in growing high content of N, not only is it difficult to incorporate N into the InGaAs QW, but the introduction of N into a QW decreases the lattice parameter of the alloy. Therefore, the strain in the layer causes its emission wavelength to shift to longer wavelengths. Furthermore, larger N concentrations broaden the luminescence linewidth of the alloys, increasing the non radiative (monomolecular and Auger) recombination, and thus lowering the material gain and increasing transparency carrier density.[9,10)] Recently, Chang *et al.* found that incorporating nitrogen at a content exceeding 0.7% in InGaAsN significantly reduced the laser characteristics and temperature of the laser performance.[9)] Consequently, understanding the influence of nitrogen in the InGaAsN QW is particularly important.

In this work, we present the results of studies on the influence of various nitrogen contents ($x = 0.5$ and 2%) on the optical properties, including the carrier localization and material properties, of $In_{0.4}Ga_{0.6}As_{1-x}N_x$/GaAs QWs. Detailed analyses of power- and temperature-dependent photoluminescence (PL) and high-resolution transmission electron microscopy (HRTEM) measurements were carried out to clarify the crystal and interface quality of InGaAsN–GaAs.

2. Experiments

All samples investigated were grown by low-pressure metalorganic chemical vapor deposition (LP-MOCVD). AsH_3 and PH_3 as hydride sources were supplied as the group-V precursors, the trimethyl precursors of gallium (Ga), aluminum (Al), and indium (In) acted as the group-III precursors, and the N precursor was U-dimethylhydrazine. The active regions were all based on a 60 Å $In_{0.4}Ga_{0.6}As_{1-x}N_x$ QW sandwiched between GaAs (100 Å)–GaAsP (75 Å) materials. A diagram of the structure is shown in Fig. 1. Moreover, the In and N contents of the InGaAsN material were determined via PL, X-ray diffraction and secondary ion mass spectrometry. The details of growth conditions have been published elsewhere.[11–13)] The values of the N composition x in the structures were 0.5 and 2% for samples A and B, respectively.

The surface morphology of the sample was determined by optical microscopy and atomic force microscopy (AFM). Roughness analysis indicated that smooth and mirror like surfaces (on the nanoscale), which are exactly like that of a GaAs homoepitaxial layer, can be achieved under optimized growth conditions. Cross-sectional TEM thin foils were prepared through mechanical polishing followed by argon-ion milling. The PL was excited by the 514.5 nm line of an

*E-mail address: hckuo@faculty.nctu.edu.tw

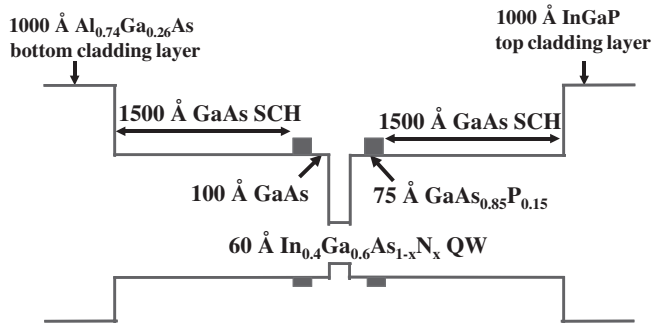

Fig. 1. Schematic structure of $In_{0.4}Ga_{0.6}As_{1-x}N_x$/GaAs SQW.

Ar^+-ion laser focused to a spot with a minimum diameter of 40 μm. All samples were placed in a closed-cycle cryostat with a temperature controller ranging from 10 K to room temperature. The luminescence was dispersed with a double-grating monochromator (Spex Triax 320) and equipped with a thermo-electrically cooled InGaAs detector.

3. Results and Discussion

The PL spectra of the excitation-power dependence of samples A and B measured at 10 K are shown in Fig. 2. The range of excitation power was from 0.2 to 27.5 mW. Figure 2(a) presents a series of spectra recorded at various excitation powers for sample A. A clear tendency of a blue shift with increasing excitation power is observed. As shown in Fig. 2(b) for sample B, only one peak appears under low excitation power, just as in sample A. However, one peak appears on the high-energy side with increasing excitation power, starting as a shoulder under an excitation power of 4 mW, and then becomes a clean peak at 0.9 eV under an excitation power of 8 mW. Finally, the peak on the high-energy side dominates over the initial peak under low excitation power (on the low-energy side). This phenomenon is most likely a feature of quantum dots (QDs) resulting from carrier localization and a more efficient recombination through QDs, which has been observed in other III–nitride semiconductor alloys.[14)]

To further explore the properties of emission, the temperature dependence of the PL was evaluated on both samples under an excitation power of approximately 27.5 mW, and the spectra are shown in Fig. 3. The variation of peak position with temperature can be attributed to the effect of the extension of the lattice and the electron lattice

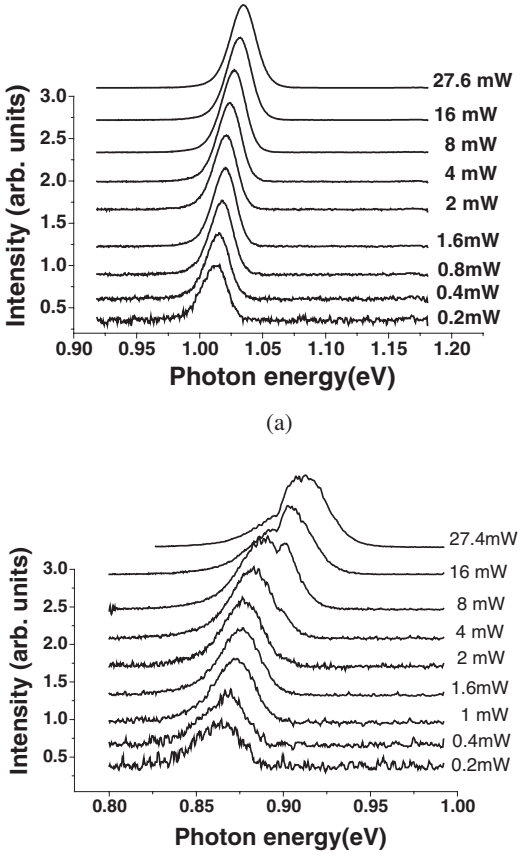

Fig. 2. Excitation-power dependent PL of (a) sample A ($In_{0.4}Ga_{0.6}As_{0.995}N_{0.005}$/GaAs SQW) and (b) sample B ($In_{0.4}Ga_{0.6}As_{0.98}N_{0.02}$/GaAs SQW).

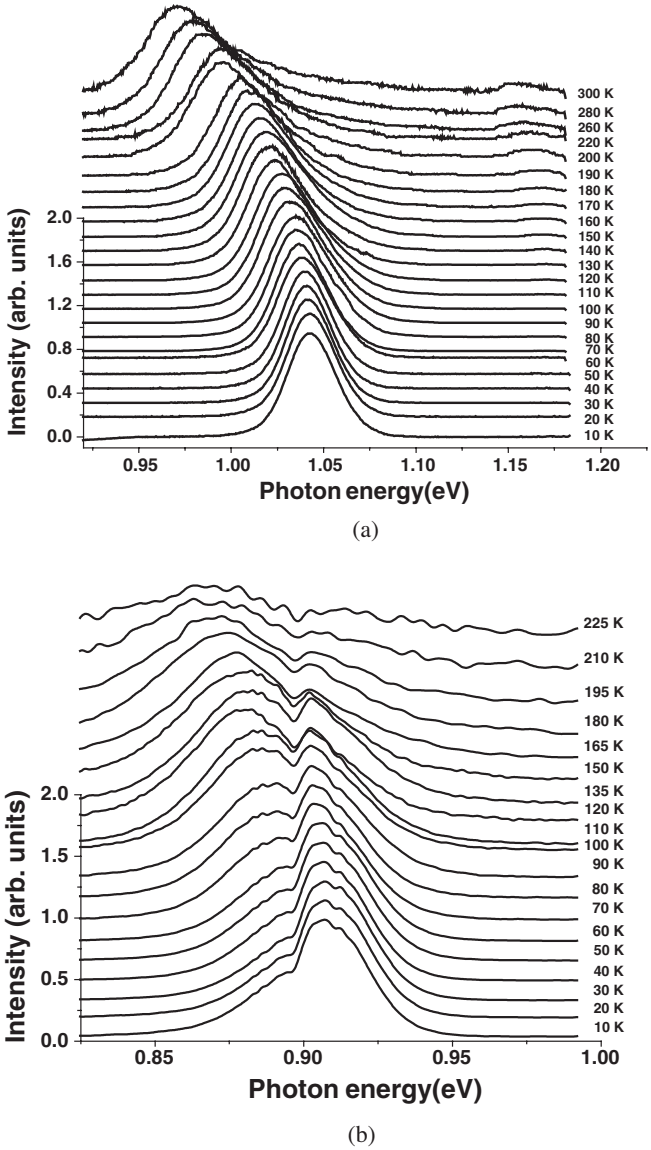

Fig. 3. Temperature-dependent PL of (a) sample A ($In_{0.4}Ga_{0.6}As_{0.995}N_{0.005}$/GaAs SQW) and (b) sample B ($In_{0.4}Ga_{0.6}As_{0.98}N_{0.02}$/GaAs SQW).

interaction. Both samples A and B clearly show remarkable broadening of their full width at half maximum (FWHM). The inhomogeneous and temperature-dependent homogenous parts are known to contribute to the luminescence broadening.[15] Figure 3(a) shows the peak in the PL emission of sample A centered at 1.042 eV with a FWHM of 30 meV at 10 K. A single symmetrical peak was observed in PL spectra when the temperature was below 190 K. As the temperature increased above 190 K, the PL spectra broadened thermally and showed a lower intensity as expected. Notably, unlike those of the symmetric low-temperature PL spectra observed for sample A, two main emission peaks were observed at 0.882 and 0.909 eV at 10 K for sample B, as showen in Fig. 3(b). As the temperature increased, the high-energy peak apparently persisted around 0.905 eV, while the low-energy peak continued to shift to lower energy (red shift). The PL emission of sample A and the low-energy band of sample B both showed the typical behavior of band-gap emission: a decrease in the emission energy with increasing temperature due to thermal expansion, which is well described by the Varshni model[16] (not shown here). The trends of both temperature insensitivity and increase in intensity with excitation power reveal that the extraordinary peak on the high-energy side of the PL emission observed in sample B may originate from quantum-dot-like states. The high emission energy of the 0.9 eV band might be due to a quantum-confined induced shift, while the persistence of the high-energy peak with temperature can be understood by considering the lower electron–phonon interaction in the dot-like structure. Nevertheless, the intensity of the high-energy peak decreased faster with temperature than both the low energy peak and the high-energy shoulder of the 0.9 eV band decreased with temperature. This thermal quenching behavior of the high-energy peak of sample B might be attributed to trapped excitons or carriers thermalizing from localized regions as a result of potential fluctuations in QD-like states. Further increases in temperature degrade the PL intensity because of the recombination of the thermally activated carriers by a nonradiative mechanism in the sample.

In order to directly investigate the crystal quality and the interface of both single-QW (SQW) samples and to obtain further evidence of the dot-like structure of sample B, high-resolution TEM (HRTEM) images were taken and are shown in Fig. 4. A very clear interface of $In_{0.4}Ga_{0.6}As_{0.995}N_{0.05}$ SQW was obtained on the atomic-layer level [Fig. 4(a)], whereas no dislocations were observed in low-magnification images. Numerous studies have reported that a suitable amount of nitrogen incorporation into InGaAs could reduce net strain.[17,18] Additionally, the HRTEM image of sample A shows very high crystallinity without extended structural defects, which is similar to the crystallinity of conventional III–V materials. Notably, for sample B with 2% nitrogen content ($In_{0.4}Ga_{0.6}As_{0.98}N_{0.02}$ SQW), small dark regions about 2–3 nm in size were formed in the interface as shown in Fig. 4(b), implying the possibility of the formation of quantum-dot like states.

The origin of quantum-dot-like states is not well understood, and there are relatively few reports of InGaAsN/GaAs QDs.[19–23] These results show experimental evidence of the three-dimensional (3D) growth mode in samples with

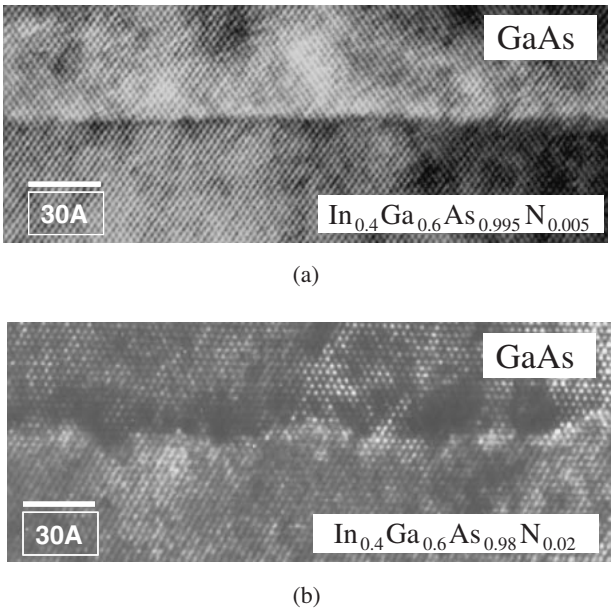

Fig. 4. High-resolution TEM images of (a) sample A ($In_{0.4}Ga_{0.6}As_{0.995}N_{0.005}$/GaAs SQW) and (b) sample B ($In_{0.4}Ga_{0.6}As_{0.98}N_{0.02}$/GaAs SQW).

2% nitrogen content. This phenomenon most likely occurs due to the influence of various nitrogen contents on growth model transitions, i.e., two-dimensional (2D) to 3D growth, to minimize the free energy while increasing the nitrogen content. Moreover, theoretical studies have shown that island formation results from the competition between strain relaxation and surface energy.[24] A crucial factor in the control of 3D island growth is the lattice mismatch among the island material, the underlying substrate and the surrounding matrix. The introduction of nitrogen into a system with high compressive strain (InGaAs and GaAs substrate) can reduce the average strain, but the local strain around N atoms may increase because of the small radius of the nitrogen atom compared with that of arsenic. The effect of this local strain may enhance the 3D growth mode. Furthermore, Herrera *et al.* proposed that the introduction of N could be responsible for the enhanced phase separation.[23] The presence of phase separation could also reduce the energy barrier locally for the transformation into stable 3D islands. From TEM, temperature- and excitation-dependent PL measurements, the 3D growth mode can be easily organized under high nitrogen content, although the mechanism of the formation of QDs in InGaAsN SQW is not yet well known. Therefore, a more detailed analysis, including thermodynamic and kinetic constraints, is required to determine whether the quantum-dot-like states are energetically favorable in InGaAsN alloys with high nitrogen content.

4. Conclusions

We have investigated TEM, temperature- and excitation-dependent PL measurements on $In_{0.4}Ga_{0.6}As_{1-x}N_x$ SQWs ($x = 0.5$ and 2%) grown by MOCVD. The $In_{0.4}Ga_{0.6}As_{0.995}N_{0.005}$ SQW shows smooth interface and good PL emission properties, which were attributed to band-to-band emissions. The peak in the PL emission of the $In_{0.4}Ga_{0.6}As_{0.995}N_{0.005}$ SQW was centered at 1.042 eV with FWHM of 30 meV at

10 K. For high nitrogen content ($x = 2\%$), the interface was rough and was observed to have dark island regions. Two peaks in the PL emission were observed at 0.882 eV and 0.909 eV at 10 K. The peak at lower energy may be from the band-to-band transition, while the higher-energy peak may be due to the quantum-dot-like state confirmed by the insensitivity to temperature in temperature-dependent PL measurements. It becomes dominant under high pumping energy which might result from carrier localization and more efficient recombination through the quantum-dot-like state. Our experimental results indicate that nitrogen not only has an influence on carrier localization but also is critical to the formation of QDs.

Acknowledgements

This work was supported in part by the National Science Council of the Republic of China (ROC) in Taiwan under contract No. NSC 93-2215-E-009-063, in by the Extend Academic Excellence Program of the ROC under contract No. NSC 93-2752-E-009-008-PAE, and in part by a MediaTek Fellowship. The authors would like to thank the Opto-Electronics and Systems Laboratories of the Industrial Technology Research Institute (ITRI) for providing experimental support.

1) N. Tansu and L. J. Mawst: IEEE Photonics Technol. Lett. **14** (2002) 444.
2) J. Wei, F. Xia, C. Li and S. R. Forrest: IEEE Photonics Technol. Lett. **14** (2002) 597.
3) E.-M. Pavelescu, T. Jouhti, M. Dumitrescu, P. J. Klar, S. Karirinne, Y. Fedorenko and M. Pessa: Appl. Phys. Lett. **83** (2003) 1497.
4) G. L. Belenky, C. L. Reynolds, Jr., D. V. Donetsky, G. E. Shtengel, M. S. Hybertsen, M. A. Alam, G. A. Baraff, R. K. Smith, R. F. Kazarinov, J. Winn and L. E. Smith: IEEE J. Quantum Electron. **35** (1999) 1515.
5) P. Savolainen, M. Toivonen, P. Melanen, V. Vilokkinen, M. Saarinen, S. Orsila, T. Kuuslahti, A. Salokatve, H. Asonen, T. Panarello, R. Murison and M. Pessa: IEEE 11th Int. Conf. InP and Related Materials, 1999, p. 99.
6) K. D. Choquette, J. F. Klem, A. J. Fischer, O. Blum, A. A. Allermann, I. J. Fritz, S. R. Kurtz, W. G. Breitland, R. Sieg, K. M. Geib, J. W. Scott and R. I. Naone: Electron. Lett. **36** (2000) 1384.
7) M. Fischer, D. Gollub, M. Reinhardt, M. Kamp and A. Forchel: J. Cryst. Growth **251** (2003) 353.
8) D. Schlenker, T. Miyamoto, Z. Chen, F. Koyama and K. Iga: IEEE 11th Int. Conf. InP and Related Materials, 1999, p. 499.
9) Y.-L. Chang, T. Takeuchi, M. Leary, D. Mars, A. Tandon, R. Twist, S. Belov, D. Bour, M. Tan, D. Roh, Y.-K. Song, L. Mantese and A. Luan: Proc. Electrochem. Soc. **2003-11** (2003) 33.
10) J. S. Wanga, A. R. Kovsha, R. S. Hsiaoa, L. P. Chena, J. F. Chenc, T. S. Layd and J. Y. Chia: J. Cryst. Growth **262** (2004) 84.
11) N. Tansu, N. J. Kirsch and L. J. Mawst: Appl. Phys. Lett. **81** (2002) 2523.
12) N. Tansu, J. Y. Yeh and L. J. Mawst: Appl. Phys. Lett. **82** (2003) 3008.
13) N. Tansu, A. Quandt, M. Kanskar, W. Mulhearn and L. J. Mawst: Appl. Phys. Lett. **83** (2003) 18.
14) T. Wang, P. J. Parbrook, W. H. Fan and A. M. Fox: Appl. Phys. Lett. **84** (2004) 5159.
15) Q. Yang, J. Chen and A. Li: J. Cryst. Growth **194** (1998) 31.
16) M. A. Pinault and E. Tournie: Appl. Phys. Lett. **78** (2001) 1562.
17) I. A. Buyanova, W. M. Chen, B. Monemar, H. P. Xin and C. W. Tu: Appl. Phys. Lett. **75** (1999) 3781.
18) S. Bank, W. Ha, V. Gambin, M. Wistey, H. Yuen, L. Goddard, S. Kim and J. S. Harris, Jr.: J. Cryst. Growth **251** (2003) 367.
19) S. Makino, T. Miyamoto, T. Kageyama, N. Nishiyama, F. Koyama and K. Iga: J. Cryst. Growth **221** (2000) 561.
20) M. Sopanen, H. P. Xin and C. W. Tu: Appl. Phys. Lett. **76** (2000) 994.
21) T. Hakkarainen, J. Toivonen, M. Sopanen and H. Lipsanen: Appl. Phys. Lett. **79** (2001) 3932.
22) K. C. Yew, S. F. Yoon, Z. Z. Sun and S. Z. Wang: J. Cryst. Growth **247** (2003) 279.
23) M. Herrera, D. Gonzalez, M. Hopkinson, P. Navaretti, M. Gutierrez, H. Y. Liu and R. Garcia: Semicond. Sci. Technol. **19** (2004) 813.
24) J. Tersoff: Phys. Rev. B **43** (1991) 9377.